

POSITION OF THE MAIN IONOSPHERIC TROUGH POLAR WALL IN MAGNETICALLY QUIET CONDITIONS ACCORDING TO DATA FROM THE IONOSPHERIC TIXIE BAY STATION AND DMSP SATELLITES

A.E. Stepanov

*Yu.G. Shafer Institute of Cosmophysical Research
and Aeronomy SB RAS,
Yakutsk, Russia, a_e_stepanov@ikfia.ysn.ru*

V.L. Khalipov

*Volunteer researcher,
Yakutsk, Russia,
khalipovvictor@mail.ru*

Abstract. The paper analyzes experimental data on the position of the polar wall of the main ionospheric trough under low geomagnetic activity at $K_p=0-1$ from measurements made at the Yakutsk chain of vertical and oblique sounding ionosondes. The northern boundary of the trough under these conditions shifts to high magnetic latitudes 67–70°. This corresponds to the position of the geophysical structure “contracted oval” or compressed oval. Critical frequencies at the polar wall of the trough have high values of about 6–8 MHz. At this time,

the DMSP satellite records intense 200–300 eV electron precipitation that can create the observed ionization in the F-region of the ionosphere.

Keywords: ionosonde, meridional chain, main ionospheric trough, polar wall, magnetically quiet conditions, contracted oval, electron density.

INTRODUCTION

Stations of the Yakutsk ionosonde chain are equipped with high-potential horizontal rhomb antennas for oblique ionospheric sounding [Aisenberg, 1962; Mamrukov et al., 1982]. The use of such an antenna system, which is combined with the vertical rhomb antenna system, significantly increases the amount of information obtained by expanding the range of probed latitudes [Vasiliev et al., 1961; Mamrukov, Zikrach, 1973; Benkova et al., 1983; Mamrukov, Filippov, 1988]. So, the Tixie Bay station, whose magnetic latitude (MLat) is 65.1°, can confidently receive reflections from the polar wall of the main ionospheric trough (MIT), located at magnetic latitudes 67–75° under quiet geomagnetic conditions.

To localize geophysical measurement data in time and space, it is necessary to have models of MIT polar wall boundaries for different geomagnetic activity levels. For example, from Aureole-2 satellite data, a model of the equatorial boundary of the diffuse auroral zone, which coincides with the MIT polar boundary, was developed for the dusk sector [Galperin et al., 1977]. Using measurements made at the Yakutsk ionosonde chain for several years, we have constructed a model of the MIT polar wall in the dawn sector [Khalipov et al., 1987]. In this work, it has been found that at low geomagnetic activity, in particular at $K_p=0+$, the MIT northern boundary shifts to magnetic latitudes 67–69°. At these latitudes and higher, there is the so-called contracted oval, or compressed oval, [Lui et al., 1976; Cummock et al., 2009; Despirak et al., 2018; Kleimenova et al., 2023a; Kleimenova et al., 2023b]. Lui et al. [1976] have shown that significant energetic plasma flows are recorded in the plasma sheet in magnetic field lines, projected onto the latitudes of the contracted oval. According to DMSP satellite measurements, intense fluxes

of penetrating electrons with energies of hundreds of electron volts are observed at ionospheric heights in the contracted oval region [Cummock et al., 2009]. Features of high-latitude polar substorms have been analyzed in [Despirak et al., 2018; Kleimenova et al., 2023a; Kleimenova et al., 2023b]. These substorms have the same characteristics as at the auroral oval latitudes, but magnetic activity is localized only at high latitudes.

In this paper, we deal with the events occurring under very quiet geomagnetic conditions when the MIT polar wall was always at the latitudes of the Tixie Bay station or to the north of it, and compare this ionospheric structure with the structure of energetic particle precipitation from simultaneous DMSP measurements.

EXPERIMENT

In [Galperin et al., 1977; Khalipov et al., 1977; Khalipov et al., 1987], data from the Aureole-2 satellite and high-latitude ionospheric stations of the Yakutsk meridional chain was used to analyze the location of the MIT polar wall in the dusk and dawn MLT sectors.

Since the geographic meridian, from which the universal time (UT) is determined, and the meridian of the local magnetic time of the Tixie Bay station almost coincide (the difference is from ~18 to 40 min), we can suppose that for the Tixie Bay station MLT and UT are the same time interval.

As shown by statistical studies [Galperin et al., 1977; Khalipov et al., 1977; Khalipov et al., 1987] based on a large data array, in the dawn sector under very quiet geomagnetic conditions ($K_p=0-1$) the position of the MIT polar wall features two branches diverging from their common approximation to the pole and equator. This can be seen in Figure 1 presented in [Khalipov et al., 1987].

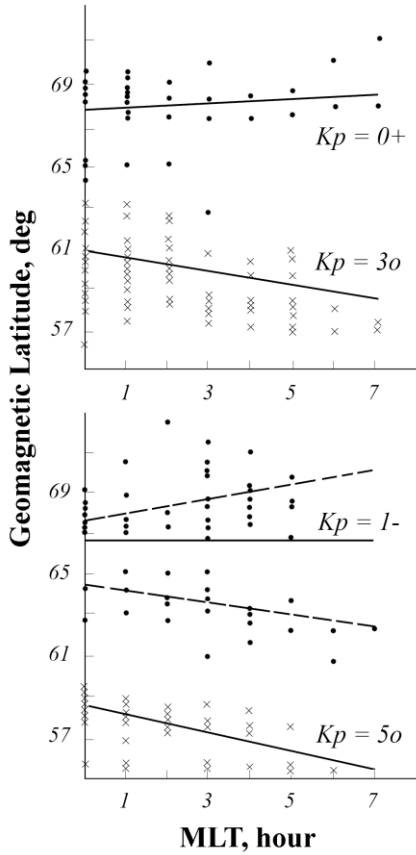


Figure 1. Magnetic latitude of the main ionospheric trough polar wall in the dawn MLT sector. Straight lines indicate approximating dependences on the K_p index

Thus, depending on external factors (such as the interplanetary magnetic field components B_y , B_x , B_z , the solar wind proton flux velocity and density, which are implica-

itly included in K_p , but have a significant effect at such small K_p), the boundary of the MIT polar wall moves with time either to the north or to the south of the observation station. This situation is illustrated in Figure 1 by the example of measurements of the location of the MIT polar wall at the Tixie Bay station (MLat=65.1°) for $K_p=1-$, i.e. under quiet geomagnetic conditions [Khalipov et al., 1987]. According to [Khalipov et al., 1987], the magnetic latitude of the MIT polar wall at different geomagnetic activity levels is empirically described by the following expression:

$$\text{MLat} = (68.9 - 3.57 K_p + 0.29 K_p^2) + (0.21 - 0.25 K_p + 0.025 K_p^2) \text{MLT.}$$

Let us examine the space-time dynamics of the MIT polar wall during geomagnetically quiet periods from ground and satellite measurements.

The left panel of Figure 2 displays a sequence of ionograms of backscatter sounding (BS) at the Tixie Bay station for the quiet day on December 9, 1983, when radio signals were reflected from large-scale ionospheric inhomogeneities to the north of the observation station. The ionograms cover an approximately 16-hour interval from 08:45 on December 9, 1983 to 00:15 UT the next day. The planetary three-hour K_p indices during this period were 2, 1, 0+, 0+, 0+, 1-, 1-, 0; $\Sigma K_p=5+$.

Note that the local midnight on the meridian of Tixie (LT=UT+9 hrs) is at 15:00 UT.

The first reflections from the MIT polar wall (F2s) and/or plasma inhomogeneities, observed in ionograms as additional traces, were recorded at 08:45 UT (17:45 LT)

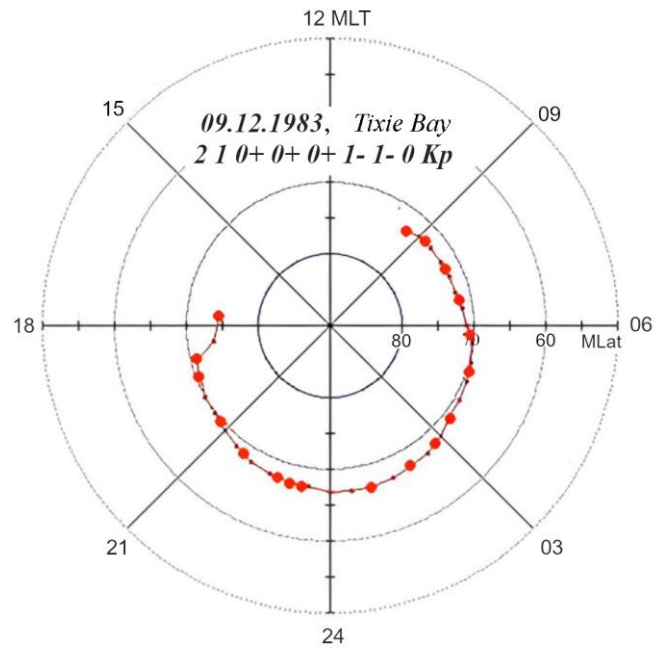
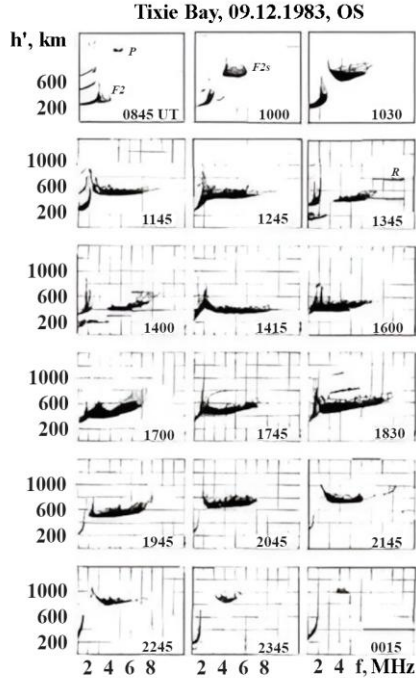


Figure 2. Sequence of ionograms of the backscatter ionospheric sounding at the Tixie Bay station for December 9, 1983 (left) and the space-time dynamics of the MIT polar wall (right) on the same day

at an altitude (range) ~ 1100 km. When recalculated to the range along the Earth surface, such a reflection corresponds to MLat $\sim 74^\circ$ (see Figure 2). Further, the reflection in the ionograms shifts downward, and at 13:45 UT it is recorded at an altitude of 400 km with a frequency ~ 8 MHz. Additional traces are clearly pronounced and are reflections at critical frequencies from inhomogeneities formed by particle precipitation in the energy range to ~ 1 keV, or by soft-energy particles [Galperin et al., 1977; Rees, 1963; Belinskaya, Khalipov, 1983]. At the same time, traces (designated as R) of auroral arcs appear in ionograms in the contracted oval region — direct stack traces without noticeable group delay near cutoff frequencies [Bates et al., 1966; Farley, 1963; Khalipov et al., 1984]. All recorded reflections from the F-region are diffuse, without distinct separation into o and x components, with a clear lower edge of the traces. Such traces in ionograms are characteristic of oblique echoes from the MIT polar wall [Khalipov et al., 1977]. The critical frequency of the regular F2 layer in the ionograms ranges from 1.5 to 4 MHz, and the layer height varies from 210 to 350 km. At 14:15 UT (23:45 LT), the frequency of sporadic reflections has a maximum ~ 10 MHz at ~ 350 km altitude, or at $\sim 68^\circ$ magnetic latitude. Then, additional reflections (plasma inhomogeneities) slowly begin to shift northward and reach $\sim 73^\circ$ magnetic latitude at 00:30 UT (09:30 LT) the next day.

The algorithm for converting the group range of reflections in ionograms to the range D along the Earth surface is given in [Mamrukov et al., 1973], in which trajectories of short radio waves were calculated by a numerical method. Note that some studies, when calculating trajectories of short radio waves in the ionosphere, made direct numerical step-by-step calculations of the angle of wave refraction by 0.1° . In the real vertical distribution of the electron density in the form of a Chapman layer, its changes are defined by the exponent, where there is also an exponent in the index. At the same time, the wave experiences weak refraction when

entering the layer, which increases as it approaches the maximum of the layer. We traced the radio wave trajectory to the region, where it became orthogonal to the local magnetic field, and determined the range along the Earth surface to this boundary.

Thus, if near the point, where the beam becomes orthogonal to the magnetic field, the ionosphere is filled with field-aligned inhomogeneities having a size of the order of wavelength, a critical reflection of radio waves from such inhomogeneities takes place. The accuracy of measuring the range D varies within ± 50 km (about half a degree of latitude).

The right panel of Figure 2 shows the space-time dynamics of the MIT polar wall on December 9, 1983 in coordinates local magnetic time — magnetic latitude. Dots mark the position of the MIT polar wall according to backscatter ionospheric sounding data from the Tixie Bay station. Larger red dots indicate the times of the ionograms presented in the left panel.

Let us analyze simultaneous ground and satellite measurements made on December 9, 1983. Figure 3 illustrates the space-time dynamics of the MIT polar wall according to Tixie Bay station data (left) and exhibits spectrograms of electron and ion precipitation obtained by the DMSP-F6 satellite (right). The black color in the left panel shows part of the satellite's trajectory; the black asterisk marks the equatorial edge of electron precipitation, which, as derived from simultaneous ground measurements, coincides with the MIT polar wall.

The black asterisk on the spectrograms (right panel) indicates the MIT polar wall at $\sim 69.1^\circ$ magnetic latitude. The same sharp edge of precipitation is seen in the dawn MLT sector (green asterisk). Since the geophysical situation is stationary, it is reasonable to make a comparison for the dawn sector too. Referring to Figure 3, the position of the MIT polar wall coincides in both space and time according to ground and satellite data.

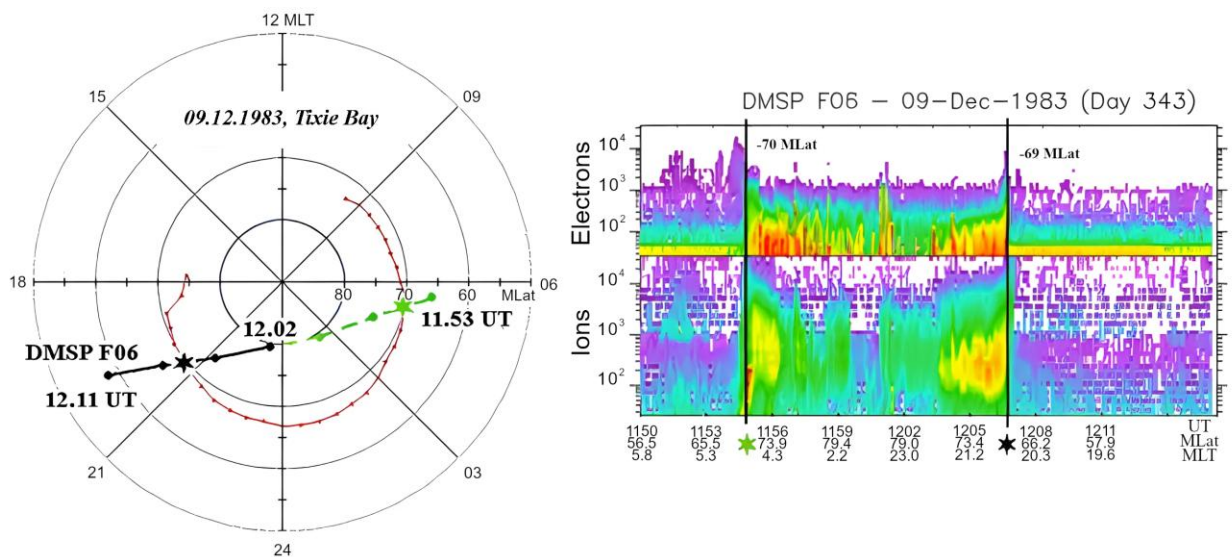


Figure 3. December 9, 1983: the DMSP-F06 satellite trajectory in MLat-MLT coordinates during its passage at ~ 12 UT (left) and spectrograms of electron and ion precipitation (right) during the passage. Asterisks mark the location of the MIT polar edge in the dusk (black) and dawn (green) sectors

Figure 4 displays spectrograms recorded by DMSP-F06 5 and 10 hrs later than the spectrograms in Figure 3. In this case, the equatorial boundary of precipitation of soft-energy particles and/or the MIT polar wall are seen to remain almost at the same latitude. This means that particle precipitation does not stop and their intensity is virtually unchanged. The same pattern is observed in the dawn MLT sector as in the dusk sector: the position of the sharp edges of electron and ion precipitation is in line with the position of clear reflections from ionospheric large-scale inhomogeneities.

Thus, the MIT polar wall and the soft-energy electron precipitation recorded by the DMSP-F06 satellite on this day spatially coincide and are observed for ~ 15 hrs.

On the same day, another satellite, DMSP-F07, took measurements over the Tixie Bay station (Figure 5). The satellite and ground measurements were synchronous near local midnight. DMSP-F07 and the Tixie Bay station detected respectively electron and ion particle precipitation and the MIT polar wall at the same magnetic latitude ($\sim 67^\circ$). The blue color in Figure 5 shows the continuation of the satellite's trajectory in the dawn MLT sector, where the MIT and particle precipitation boundaries are also seen to coincide, i.e. in this case, there is also agreement between satellite and ground measurements.

Unfortunately, for the next day we considered, December 4, 2004 (Figure not shown), there was no data on the K_p index, but according to SuperMag data [Gjerloev, 2009, 2012; Newell, Gjerloev, 2014] the day was geomagnetically quiet. When passing in the early dusk sector ($\sim 16:30$ MLT), the DMSP-F13 satellite detected soft-energy electron precipitation near the magnetic lati-

tude of 72° . The MIT polar wall was detected by the Tixie Bay station from 21:00 LT (12:00 UT) to 08:00 a.m. at magnetic latitudes 67 – 72° . Thus, in this case the MIT polar wall was observed for a long time under quiet geomagnetic conditions.

On December 24, 2004 (Figure 6), geomagnetic conditions were also quiet: the three-hour K_p indices were $1-$, 0 , $0+$, $0+$, 1 , 2 , $1-$, $1+$; $\Sigma K_p = 6+$. The DMSP-F15 and F16A satellites crossed the MIT polar wall at 18 – 19 MLT. Unfortunately, we cannot demonstrate the pattern of precipitation in the dawn sector since the satellites' trajectories did not cross it, but when measured from the ground the MIT polar wall was observed until 9 LT. In the dusk sector, according to data from the Tixie Bay station, the MIT polar wall was seen until 22:30 LT (red dots in Figure 6). The Tixie Bay station recorded reflections only from the E layer until 06:00 LT, i.e. the so-called condition A was formed — shielding of the overlying F layer by the underlying E layer [URSI Manual, 1977; Instruction, 1985]. In ionograms from the Tixie Bay station, traces of $F2_s$ reflections from the MIT polar wall are again detected after 6 LT, when an increase in the height of reflections clearly indicates the northward motion of this structure.

From 22:30 LT, the vertical sounding station Zhigansk begins observing the MIT polar wall (black circles in the left panel of Figure 6). The polar wall is seen to the north of the Zhigansk station all night, and in the morning it shifts to high magnetic latitudes. Figure 6 on the right presents a spectrogram of electron precipitation and ion density variations (top), as well as the Zhigansk station's ionograms (bottom) recording additional traces of reflections from the northern radio sounding quadrant. The red color of reflections in the ionograms indicates the arrival of radio signals from the zenith of the observation station; the blue color of reflections implies the arrival of radio signals from northern quadrants.

The ionograms from the Zhigansk station show that at 14:30 UT additional reflections, highlighted in blue (coming from the north), are recorded at an altitude ~ 590 km, which, when recalculated to the Earth range, approximately corresponds to the latitude of the Tixie Bay station. The next two ionograms indicate that the reflected signals continue to come from the north, but the region of their reflection approaches the observation station.

DISCUSSION

The polar wall of the main ionospheric trough coincides with the equatorial boundary of electron precipitation (Khalipov et al., 1977). The spectral distribution of electrons in the diffuse auroral zone is illustrated in [Belinskaya, Khalipov, 1983], where the vertical density profile in the F-region is calculated for it. Ground-based ionospheric measurements, as well as measurements from the DMSP-F6, -F7, -F15, and -F16A satellites, carried out in the contracted oval region on December 9, 1983, December 4, and December 24, 2004 during geomagnetically quiet periods, reveal significant fluxes of precipitating electrons (see Figures 3–6). The spectral

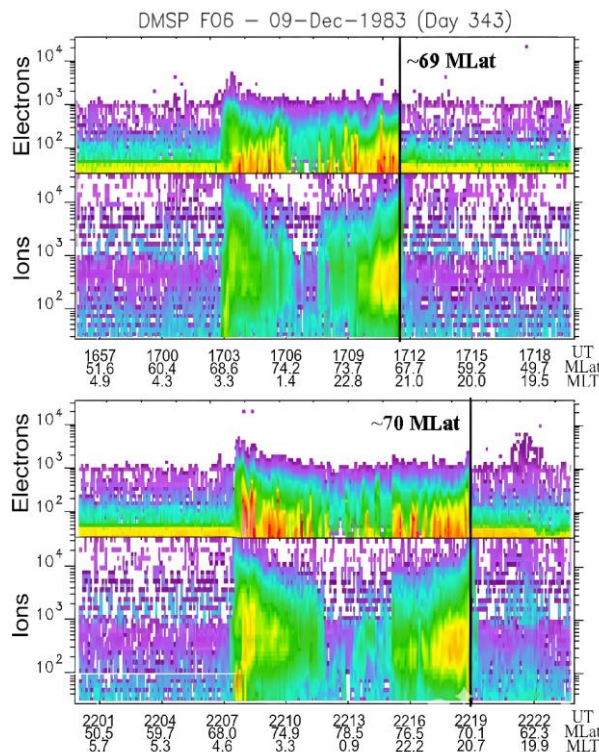


Figure 4. Spectrograms recorded by DMSP-F06 respectively ~ 5 (top) and 10 (bottom) hrs later than the spectrograms in Figure 3. Vertical black lines indicate the position of the trough polar wall

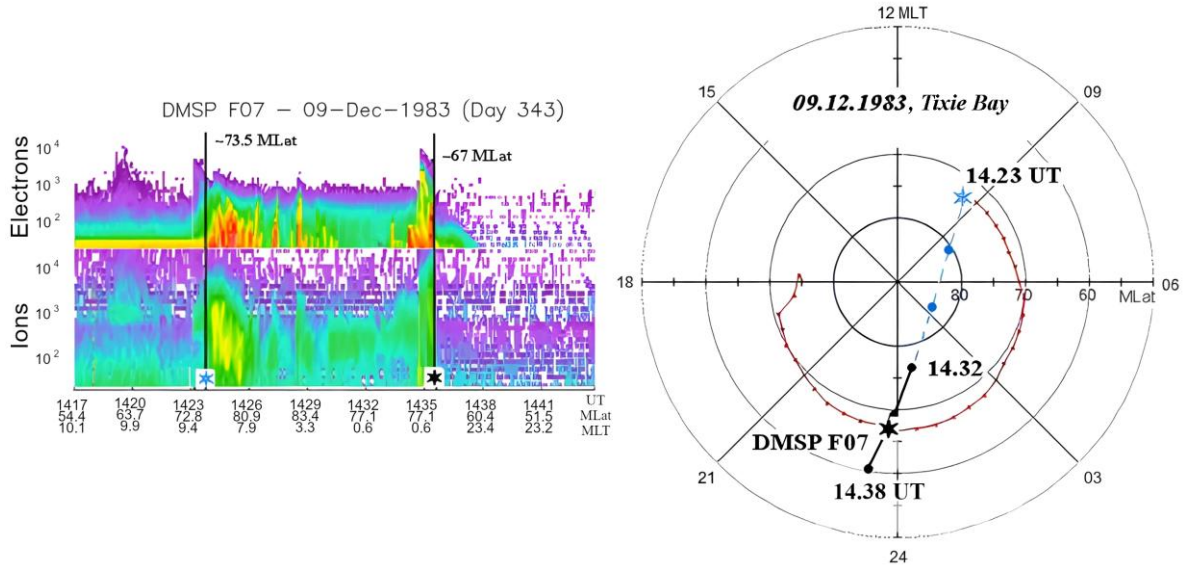


Figure 5. December 9, 1983: DMSP-F07 satellite trajectory in MLat–MLT coordinates (right) and spectrograms of electron and ion precipitation (left) during its passage

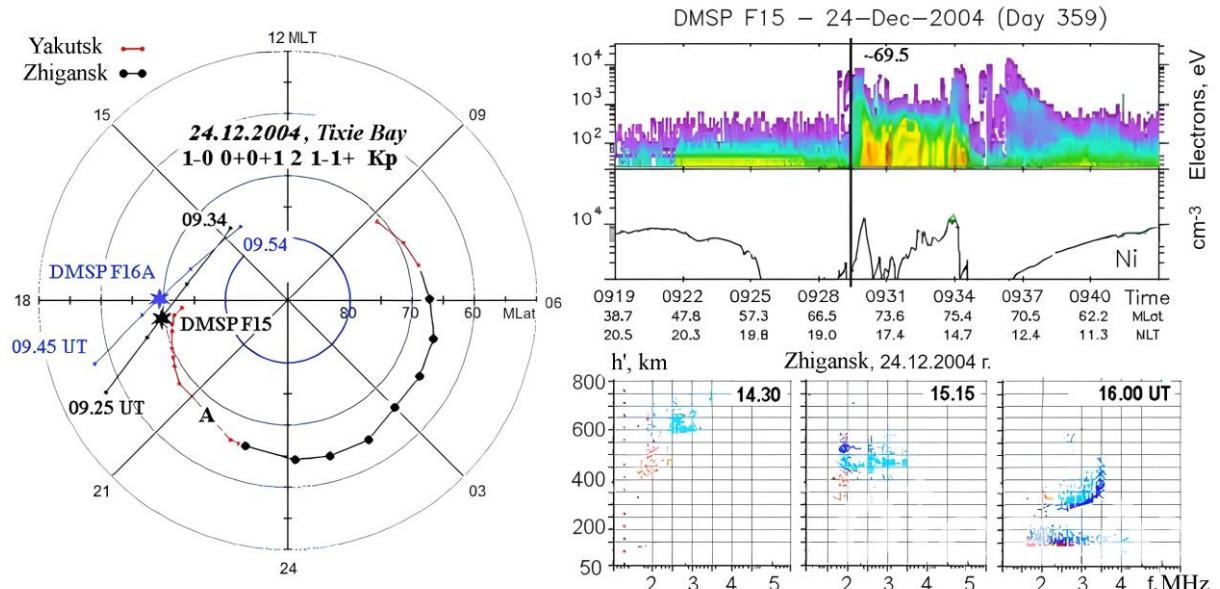


Figure 6. December 24, 2004: on the left are the DMSP-F15 and-F16A trajectories and the position of the MIT polar wall as measured at the Tixie Bay (red dots) and Zhitgansk (black dots) stations in MLat–MLT coordinates; on the right is the spectrogram of electron precipitation and ion density variations (top) as well as the Zhitgansk station's ionograms recording the MIT polar wall (bottom). The black vertical line on the spectrogram indicates the equatorial edge of electron precipitation

distribution maximum covers the range from hundreds of electron volts to 1 keV. Particles with such energy can create significant ionization in the F-region. In all cases of simultaneous satellite and ground measurements, the MIT polar wall coincides with the equatorial boundary of particle precipitation.

Detailed characteristics of precipitating electrons under similar quiet geomagnetic conditions as measured by DMSP-F13 have been studied in [Cummock et al., 2009]. Particles penetrate not only in the contracted oval region, but also in the polar cap region. Measurements of the auroral glow in the ultraviolet spectrum by the same satellite supplement the spatio-temporal picture of

the development of auroral structures. The integral flux of soft-energy electrons is 10^9 eV/(cm² s sr). The DMSP satellite data presented in our work agrees well with these results.

In the electron spectrum in the diffuse auroral zone, along with the soft-energy component there are electrons with energies to several keV. For this spectral distribution, Belinskaya and Khalipov [1983] calculated ionization profiles in the ionosphere, which suggest that the electron density in the F-region increases to $\sim(2\div3)\cdot10^4$ cm⁻³ ($f=4\div5$ MHz). However, according to measurements at the contracted oval latitudes, electron fluxes in the soft-energy spectrum in the diffuse auroral

zone are much higher. This creates the observed density level $\sim(4\div8)\cdot10^4$ cm $^{-3}$ ($f=6\div8$ MHz) on the MIT polar wall under quiet geomagnetic conditions.

We can conclude that during geomagnetically quiet periods the MIT polar wall is often detected with high-latitude ionosondes/digisondes. At the same time, the question about mechanisms of generation of such long-term precipitation from the magnetotail into the polar ionosphere remains unanswered.

CONCLUSION

Direct comparisons between ground-based ionosonde measurements and satellite data on precipitation of electrons and ions under quiet geomagnetic conditions have shown:

- According to ground-based data, the position of the main ionospheric trough polar wall closely matched the position of the equatorial boundary of soft-energy particle precipitation as measured by the DMSP satellites in the contracted oval region.
- The intensity of precipitating particle fluxes is high enough to cause an increase in the ionization of the F2-region to a level that is detected by a ground ionosonde.
- The precipitation region forming the main ionospheric trough polar wall exists for many hours in the night sector. Such behavior under quiet geomagnetic conditions raises questions about sources of soft-energy particle precipitation at high latitudes.
- From the spectrum and intensity of electron fluxes observed on the ionospheric trough polar wall under very quiet geomagnetic conditions we can conclude that they are similar to the particle population in the dayside polar cusp.

The work was financially supported by the Russian Science Foundation (Project No. 25-17-20002).

We are grateful to the NOAA/NESDIS National Geophysical Data Center for DMSP satellite data, as well as to the World Data Center for Geomagnetism in Kyoto [<http://wdc.kugi.kyoto-u.ac.jp>] and the World Agency SuperMag [https://supe_rmag.jhuapl.edu/info/] for data on geomagnetic activity indices.

REFERENCES

Aisenberg G.Z. *Korotkovolnovye antenny* [Short-wave antennas]. Moscow, Svyazizdat, 1962, 110 p. (In Russian).

Bates H.F., Belon A.E., Romick G.J., Stringer W.J. On the correlation of optical and radio auroras. *J. Atmos. Terr. Phys.* 1966, vol. 28, pp. 439–442. DOI: [10.1016/0021-9169\(66\)90053-5](https://doi.org/10.1016/0021-9169(66)90053-5).

Belinskaya S.I., Khalipov V.L. Some aeronomic effects in the aurora diffuse zone. *Issledovaniya po geomagnetizmu, aeronomii i fizike Solntsa* [Research on Geomagnetism, Aeronomy and Solar Physics]. 1983, vol. 63, pp. 116–124. (In Russian).

Benkova N.P., Zikrach E.K., Kozlov E.F., Mamrukov A.P., Osipov N.K., Samorokin N.I., Filippov L.D. Main ionospheric trough from data of meridional probe chains. *Ionosfernye issledovaniya* [Ionospheric studies]. 1983, vol. 35, pp. 5–12. (In Russian).

Cummock J.A., Blomberg L.G., Kullen A., Karlsson T., Sunberg K.A. Small-scale characteristics of a extremely high latitude aurora. *Ann. Geophys.* 2009, vol. 27, pp. 3335–3341. DOI: [10.5194/angeo-27-3335-2009](https://doi.org/10.5194/angeo-27-3335-2009).

Despirak I.V., Lubchich A.A., Kleimenova N.G. High-latitude substorm dependence on space weather conditions in solar cycle 23 and 24 (SC23 and SC24). *J. Atmos. Solar-Terr. Phys.* 2018, vol. 177, pp. 54–62. DOI: [10.1016/j.jastp.2017.09.011](https://doi.org/10.1016/j.jastp.2017.09.011).

Galperin Yu.I., Cranier J., Lissakov Yu.V., Nikolaenko L.M., Sinitsyn V.M., Sauvaud J.-A., Khalipov V.L. Diffuse auroral zone. I. Model of the equatorial boundary of the diffuse zone of auroral electron invasion in the evening and near-midnight sectors. *Kosmicheskie issledovaniya* [Cosmic Res.]. 1977, vol. 15, no. 3, pp. 421–434. (In Russian).

Farley D.T., Jr. A plasma instability resulting in field-aligned irregularities in the ionosphere. *J. Geophys. Res.* 1963, vol. 68, pp. 6083–6097. DOI: [10.1029/JZ068i022p06083](https://doi.org/10.1029/JZ068i022p06083).

Gjerloev J.W. A Global Ground-Based Magnetometer Initiative. *EOS*. 2009, vol. 90, pp. 230–231. DOI: [10.1029/2009EO270002](https://doi.org/10.1029/2009EO270002).

Gjerloev J.W. The SuperMAG data processing technique. *J. Geophys. Res.* 2012, vol. 117, A09213. DOI: [10.1029/2012JA017683](https://doi.org/10.1029/2012JA017683).

Instruktsiya po obrabotke ionogramm naklonnogo zondirovaniya [Instructions for processing oblique sounding ionograms]. Ed. Vinogradova Yu.V. Leningrad, Gidrometeoizdat, 1985, 127 p. (In Russian).

Khalipov V.L., Galperin Yu.I., Lissakov Yu.V., Cranier J., Nikolaenko L.M., Sinitsyn V.M., Sauvaud J.-A. Diffuse auroral zone. II. Formation and dynamics of the polar edge of the subauroral ionospheric trough in the evening sector. *Kosmicheskie issledovaniya* [Cosmic Res.]. 1977, vol. 15, no. 5, pp. 708–724. (In Russian).

Khalipov V.L., Golenkov E.V., Molochushkin N.E., Stepanov A.E. Characteristic traces on oblique incidence-backscatter sounding ionograms during the appearance of auroral arcs. *Byulleten nauchno-tehnicheskoi informatsii. Problemy kosmofiziki i aeronomii* [Bull. of Scientific Technology Information. Problems of Cosmophysics and Aeronomy]. Yakutsk, USSR SB SA Publ., 1984, pp. 33–35. (In Russian).

Khalipov V.L., Stepanov A.E., Novopashina E.Yu. Model of the position of the polar edge of the ionospheric trough in the morning sector. *Geomagnetizm i aeronomiya* [Geomagnetism and Aeronomy]. 1987, vol. 27, no. 5, pp. 842–843. (In Russian).

Kleimenova N.G., Gromova L.I., Despirak I.V., Malysheva L.M., Gromov S.V., Lubchich A.A. Features of polar substorms: An analysis of individual events. *Geomagnetism and Aeronomy*. 2023a, vol. 63, no. 3, pp. 288–299. DOI: [10.1134/S0016793223600042](https://doi.org/10.1134/S0016793223600042).

Kleimenova N.G., Despirak I.V., Malysheva L.M., Gromova L.I., Lubchich A.A., Roldugin A.V., Gromov S.V. Substorms on a contracted auroral oval. *J. Atmos. Solar-Terr. Phys.* 2023b, vol. 245, p. 106049. DOI: [10.1016/j.jastp.2023.106049](https://doi.org/10.1016/j.jastp.2023.106049).

Lui A.T.Y., Akasofu S.-I., Hones E.W., Bame S.J., McIlwain C.E. Observation of plasma sheet during a contracted oval substorm in a prolonged quiet period. *J. Geophys. Res.* 1976, vol. 81, pp. 1415–1419. DOI: [10.1029/JA081i007p01415](https://doi.org/10.1029/JA081i007p01415).

Mamrukov A.P., Zikrach E.K. Morphology of subauroral F2s. *Geomagnetizm i aeronomiya* [Geomagnetism and Aeronomy]. 1973, vol. 13, pp. 433–436. (In Russian).

Mamrukov A.P., Filippov L.D. Yakutsk meridional chain of ionosondes for vertical and oblique incidence-backscatter sounding and round-the-clock observations of the main ionospheric failure. *Effekty vysypaniya zaryazhennykh*

chastits v verkhnei atmosfere [Effects of charged particle ejection in the upper atmosphere]. Yakutsk, YaF SB AS USSR Publ., 1988, pp. 107–123. (In Russian).

Mamrukov A.P., Khalipov V.L., Filippov L.D. Calculation of ionograms for rakurs-sensitive reflections from the ionosphere. *Geofizicheskie yavleniya v polyarnoi oblasti* [Geophysical phenomena in the polar region]. Yakutsk, YaF SB AS USSR Publ., 1973, pp. 92–97. (In Russian).

Mamrukov A.P., Kiselev V.A., Neustroev E.M., Filippov L.D. Combined ionosonde for vertical and oblique incidence-backscatter sounding for diagnostics of the ionosphere at the latitudes of the plasmapause in Zhigansk. *Byulleten nauchno-tehnicheskoi informatsii. Problemy kosmofiziki i aeronomii* [Bull. of Scientific Technology Information. Problems of Cosmophysics and Aeronomy]. Yakutsk, YaF SB AS USSR Publ., 1982, pp. 24–27. (In Russian).

Newell P.T., Gjerloev J.W. Local geomagnetic indices and the prediction of auroral power. *J. Geophys. Res.* 2014, vol. 119, pp. 9790–9803. DOI: [10.1002/2014JA020524](https://doi.org/10.1002/2014JA020524).

Rees M.H. Auroral ionization and excitation by incident energetic electrons. *Planetary and Space Science*. 1963, vol. 11, no. 10, pp. 1209–1218.
DOI: [10.1016/0032-0633\(63\)90252-6](https://doi.org/10.1016/0032-0633(63)90252-6).

Rukovodstvo URSI po interpretatsii i obrabotke ionogramm [URSI Handbook of ionogram interpretation and reduction]. Trans. from English. Ed. N.V. Mednikova. Moscow, Nauka Publ., 1977, 342 p. (In Russian).

Vasiliev G.V., Vasiliev K.N., Goncharov L.P. Automatic panoramic ionospheric station of the AIS type. *Geomagnetizm i aeronomiya* [Geomagnetism and Aeronomy]. 1961, vol. 1, no. 1, pp. 120–125. (In Russian).

URL: <http://wdc.kugi.kyoto-u.ac.jp> (accessed September 3, 2025).

URL: <https://supermag.jhuapl.edu/info/> (accessed September 3, 2025).

Original Russian version: Stepanov A.E., Khalipov V.L. published in *Solnechno-zemnaya fizika*. 2025, vol. 11, no. 4, pp. 64–70. DOI: [10.12737/szf-114202506](https://doi.org/10.12737/szf-114202506). © 2025 INFRA-M Academic Publishing House (Nauchno-Izdatelskii Tsentr INFRA-M).

How to cite this article

Stepanov A.E., Khalipov V.L. Position of the main ionospheric trough polar wall in magnetically quiet conditions according to data from the ionospheric station Tixie and DMSP satellites. *Sol.-Terr. Phys.* 2025, vol. 11, iss. 4, pp. 57–63. DOI: [10.12737/stp-114202506](https://doi.org/10.12737/stp-114202506).